

Studies on Some Infrared Stimulable Phosphors

S. P. KELLER, J. E. MAPES,* AND G. CHEROFF

Research Center, International Business Machines Corporation, Poughkeepsie, New York

(Received May 27, 1957)

Physical properties of the two phosphor systems SrS:Ce,Sm, and SrS:Eu,Sm, as well as the base material SrS, have been studied. The optical studies concern spectra of transmission, excitation, fluorescence, phosphorescence, stimulation, and stimulated emission. Relative storage efficiencies of the major exciting wavelengths have been measured. Time characteristics of the phosphorescence and the infrared exhaustion have been determined. The dc photoconductive response as a function of the wavelength of the incident light has been studied. A simplified band-theory model which correlates all of the experimental data in conjunction with the electronic structures of the activators is presented.

INTRODUCTION

THE existence of infrared stimulable phosphors has been known for a number of years. The most efficient of these storage phosphors have been found among the doubly activated alkaline-earth sulfides and selenides, zinc sulfides and selenides, and cadmium sulfides and selenides. There have been investigations of some chemical and physical properties in the past. The present work has been undertaken to obtain more basic information about these materials and to get a better working knowledge of them. The materials we investigated were SrS:Ce, Sm, SrS:Eu, Sm, and the base material SrS. These phosphors were chosen because of their great sensitivity, storageability, and rapid time response. The various measurements necessitated several types of samples and special care had to be taken in fabrication. The chemical and sample preparation will be discussed in the appendix.

The over-all instrumentation is shown and discussed in the appendix. The optical instrumentation has equipped us with considerable versatility which has allowed us to make diversified measurements including studies of transmission, excitation, fluorescence, phosphorescence, stimulation, and stimulated emission. Some of our measurements duplicate those that other workers have made.¹⁻⁸ We have made them with a great amount of thoroughness which our instrumentation has provided us. As a result, we were able to study certain optical effects that have not been studied before. Such effects are various structure features of emissions and excitations which we have tried to relate to the constituency of the phosphors. Further, the instrumenta-

tion has allowed us to make measurements that have not been made elsewhere to our knowledge. One such measurement involves the determination of the phosphorescent spectrum as a function of time lapse following excitation. This has enabled us to draw certain conclusions about the existence of thermal traps and about relative rates of those electron-hole recombinations that lead to optical emissions. Another new measurement involves the relative storageability as a function of the wavelength of exciting light which information can be correlated with photoconductivity and time measurements. The measurement of the wavelength dependence of photoconductivity has enabled us to make statements about possible mechanisms for optical processes. We have been able to complement each measurement with other different measurements, and we have been able to correlate all of the experimental results into one over-all self-consistent picture.

This report is divided into two parts. Part I describes the experimental results. Part II presents the conclusions of the work which include a simplified band-theory model of the phosphors.

I. EXPERIMENTAL RESULTS

A. Optical Studies

The instrumentation is depicted in Fig. 15 and the operation is outlined in Table III of the appendix. For the sake of notational brevity, SrS:Ce,Sm will be designated as S-1 and SrS:Eu,Sm as S-2. In the following figures, a comparison of the intensities of the different spectra is not meaningful except where stated to the contrary.

1. Excitation Spectra

These spectra were obtained when the Perkin-Elmer (PE) 98 monochromator was set at a particular wavelength (490 and 616 m μ for S-1; 595 and 645 m μ for S-2) in the fluorescent emission region of the materials, while the PE 112U was scanned. The results are presented in Fig. 1. It should be noted that the relative peak heights for any one phosphor, or base material, are meaningful in that they have been corrected for constant number of exciting photons. A comparison of peak heights of different samples is not meaningful.

* Now at Brookhaven National Laboratory, Upton, New York.

¹ University of Rochester, Report on Phosphors, Institute of Optics, 1945 (unpublished).

² R. Ward, Brooklyn Polytechnic Institute, "Preparation of IR Phosphors," 1945 (unpublished).

³ B. O'Brien, J. Opt. Soc. Am. **36**, 369 (1946).

⁴ J. J. Dropkin, Report on Photoconduction in Phosphors, 1953 (unpublished).

⁵ R. C. Herman and C. F. Meyer, J. Opt. Soc. Am. **39**, 729 (1949).

⁶ Scott, Thompson, and Ellickson, J. Opt. Soc. Am. **39**, 64 (1949).

⁷ Urbach, Nail, and Pearlman, J. Opt. Soc. Am. **39**, 675 (1949).

⁸ R. T. Ellickson and W. L. Parker, Phys. Rev. **70**, 290 (1946).

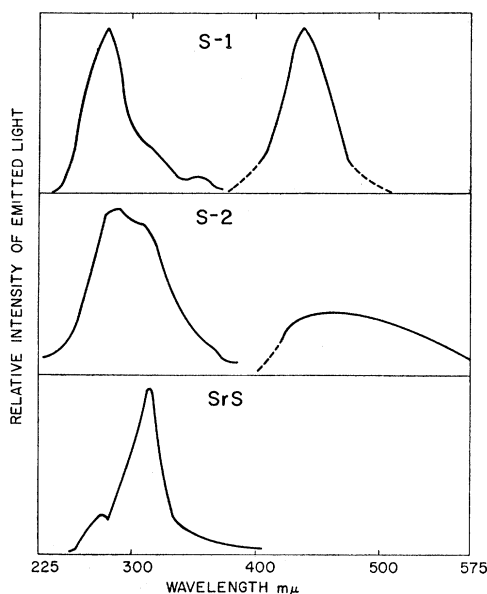


FIG. 1. Excitation spectra.

The emission from the base material is presumably due to impurities present, perhaps Cu. We had purified SrS to the extent that spectrographic analysis showed no trace of Cu. This sets the upper limit of the Cu at 1 part in 10^7 . It has been reported that Cu in this or smaller amounts is effective in causing fluorescent emission. The base-material emission might also be due to crystal imperfections, such as ion vacancies.

We propose that the 280- $m\mu$ peak in the SrS curve of Fig. 1 is due to an absorption by the base material with the emission resulting from a recombination in an impurity center. There is evidence that there occurs in this process some band-to-band recombination leading to edge emission peaked at 380 $m\mu$. Further, we propose that the peak at 315 $m\mu$ is due to an excitation of an electron from the impurity center itself into the conduction band. We also suggest that the hole thus created remains trapped in the ionized impurity center, and that recombination takes place within the center giving an emission peaked at about 490–520 $m\mu$. This emission, caused by an absorption peaked at 315 $m\mu$, is found in all of our samples, including phosphors, as can be seen in Fig. 1.

In the case of S-2, it was shown that an excitation peak at 364 $m\mu$, different from those shown in Fig. 1, could be obtained if the PE 98 monochromator were set at 452 $m\mu$. We suggest that this excitation and emission are due to an excitation of an unknown impurity center (perhaps Eu^{+3}) with subsequent recombination within this center. The intensity of this emission is less than one-tenth of the intensity of the 280- $m\mu$ excited emission and we shall make no further mention of it. It was also shown that the peak positions of the emissions varied as the wavelength of exciting light was varied. Hence,

the usual method of obtaining excitation spectra, i.e., the measurement of the intensity of one narrow band of emitted light as a function of the wavelength of incident light, is not too meaningful. This means that excitation spectra are of only general and qualitative use. A more meaningful measurement is one in which the total fluorescent emission is determined at different but closely spaced exciting wavelengths. This type of systematic investigation will be described in the next paragraph.

2. Fluorescence Studies

It is difficult to put into words descriptions of structure features of spectra without tediously repeating wavelength locations. Because of this difficulty, we shall use the words peak, shoulder, and spike in an attempt to describe various structure characteristics of the spectra. We shall ascribe the word peak to broad maxima in the spectra, whereas shoulder will be used to describe a flattening in which the slope decreases but does not become negative. The word spike will be reserved for a sharp, narrow maximum in the spectrum. The distinction between spike and peak lies only in the relative widths of the maxima. We shall associate these features with wavelengths wherever clarity requires it.

Emission spectra were determined with the exciting wavelength spaced at about every 100 Å. Figures 2(a)–(c) present some of the results. It is interesting to note the gradual transition of the general shape of the uv-excited fluorescence into the general shape of the blue-excited fluorescence. There are several excitations and emissions which had escaped detection in excitation runs, but which were discovered in the systematic investigation.

An example of this is the emission peaked at 380 $m\mu$ for 254-, 265-, and 280- $m\mu$ excitations of SrS. This could be edge emission as explained before. This emission is not seen at wavelengths between 313 and 354 $m\mu$ because of the very great preponderance of the 500- $m\mu$ emission whose peak excitation occurs at about 315 $m\mu$. As we stated before, we believe that this emission results from an ionization of some impurity center with the hole remaining trapped at the center. If we were able to amplify the short-wavelength region of the emission curve, we would perhaps see some of the 380- $m\mu$ emission. This has not been attempted. The same consideration could be applied to the 400- $m\mu$ emission caused by 344- and 354- $m\mu$ excitation of S-1. The displacement could result from low-lying trapping levels in the case of the phosphor, leading to longer wavelength "band to band" transitions. The inclusion of trapping centers, as in the case of S-1 and S-2, causes edge emission to become far less probable and it could change the spectral regions in which the emission is excited.

There is sometimes a certain small amount of irreproducibility between different samples of the same

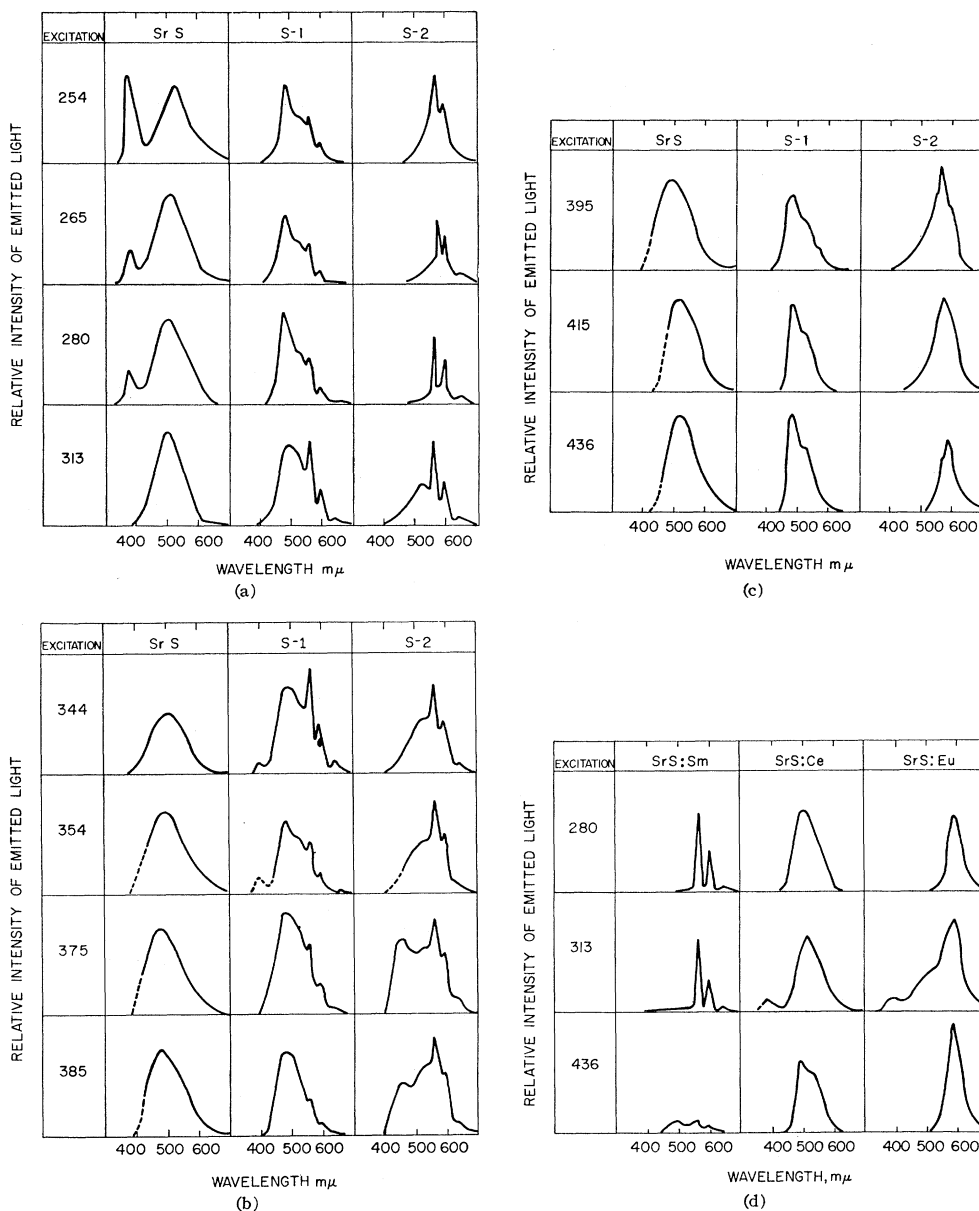


FIG. 2. (a) Fluorescence spectra. 2(b) Fluorescence spectra. 2(c) Fluorescence spectra. 2(d) Fluorescent spectra of singly activated samples. The ratio of fluorescence of SrS:Sm at 436 $m\mu$ to that at 313 $m\mu$ is 1:16 whereas, for an average low-fired S-2 phosphor, the ratio is about 4:1.

phosphor. This irreproducibility is manifested by slight shifts in peak positions, inclusions of small humps or peaks in certain samples, or changes in relative intensities of different parts of the emission spectrum. Perhaps slight shifts in emission peaks could be explained by the influence of strong base-material emissions. An example of this is the strong emission of SrS peaked between 490 and 520 $m\mu$, dependent on the exciting wavelength, as shown in Figs. 2(a)–(c). According to Fig. 1, this emission is excited more at about 315 $m\mu$ than at other wavelengths. As a result, one might expect

this emission to be most effective at changing the shape of the emission spectra for the phosphors when excited by 313- $m\mu$ light. This is seen to be true in Fig. 2(a), where the fluorescence excited by 313 $m\mu$ for S-1 and S-2 is different from the fluorescence excited by 280 $m\mu$ or by 354 $m\mu$. The difference can be explained by adding an emission, peaked at about 500 $m\mu$, to the emission curves excited by 280- $m\mu$ radiation. The inclusion of small peaks might be due to extraneous impurities or crystal imperfections and ion vacancies incorporated during the firing of the sample. The appendix

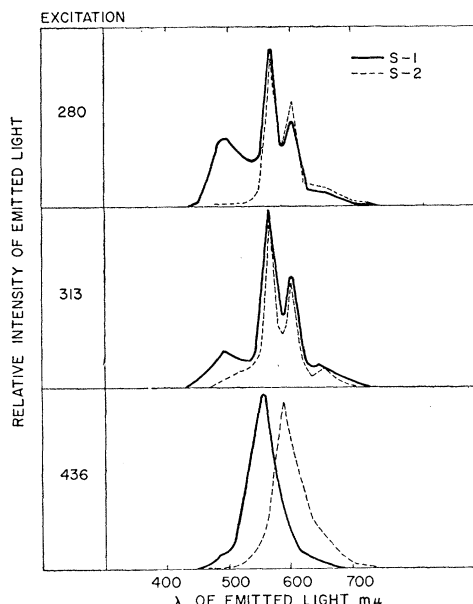


FIG. 3. Phosphorescent spectra.

describes the change in relative intensities of different parts of the emission spectrum brought about by grinding the sample. Changes of this nature could be explained on the basis of the inclusion of crystal imperfections. The imperfections could trap holes or electrons, and thus enhance or suppress one particular transition relative to another. We have not excessively concerned ourselves with these small irreproducibilities since they are beyond the scope of this investigation. There have always been dominant features common to all sample

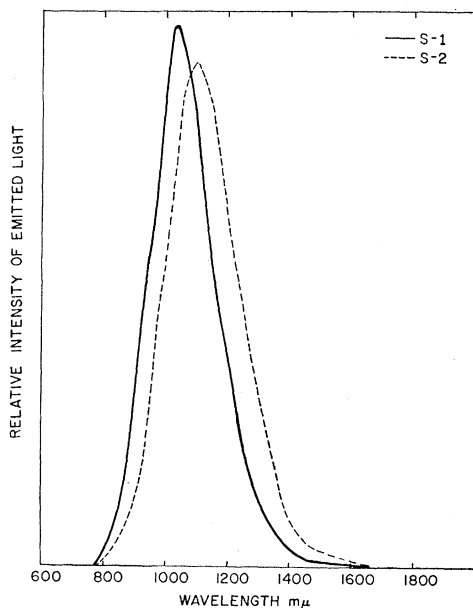


FIG. 4. Stimulation spectra.

spectra, and it has been these features which have engaged our attention.

It should be noted that in the case of *S-2*, some samples were fired at 1400°C (to be called high-fired samples). The 590- $m\mu$ emission of these samples was so strong as to obscure the spikes located at 568, 600, and 650 $m\mu$. As a result, the uv-excited fluorescence showed mainly a 590- $m\mu$ peak [to be contrasted with *S-2* of Fig. 2(b)] and the visible excited fluorescence showed only the 590- $m\mu$ peak [to be contrasted with the trace of spikes in *S-2* in Fig. 2(c)].

Samples containing only one activator but with the same concentration of flux were prepared under conditions similar to those involved in the preparation of *S-1* and *S-2*. The fluorescent spectra of these were measured so that validity could be afforded to the unique association of certain spectral features to certain activators. This association is presented in the conclusion and the spectra are shown in Fig. 2(d). Once again those small peaks located at 400 $m\mu$ are perhaps due to edge emission.

3. Phosphorescent Emission

To obtain these spectra, the sample disk of Fig. 15 was rotated as listed in Table III. The length of time between excitation and observation was dependent on the rotational frequency of the disk. In the present paragraph, we are describing the emission spectra obtained with the use of a fixed-time lapse. The spectra as a function of time lapse will be described in a later section. The phosphorescent spectra have been determined separately for the major exciting wavelengths. These spectra have the same general shape as the corresponding fluorescent spectra and they are shown in Fig. 3.

In the case of *S-1*, the main peak in Fig. 3 is at 556 $m\mu$ which probably represents the shoulder of the normal fluorescence curve when not overlapped by the 490- $m\mu$ peak. The 490- $m\mu$ peak is apparently faster than the shoulder and as a result the shoulder shows up almost alone, in Fig. 3, at 556 $m\mu$ whereas the 490- $m\mu$ peak is apparent in the phosphorescence only as a slight structure. Elsewhere in the report the shoulder is treated as being located at 533 $m\mu$. This difference has no important bearing on the results of this paper and will not be discussed again.

4. Stimulation Spectra

To effect this determination we had to overcome the difficulty of the exhaustion of the sample which occurred continuously during the run. We did this by continuously exciting the sample with a second polychromatic uv source at a spot, other than the viewing spot, as listed in Table III. In this way, a constant level of stored energy was maintained. The results are shown in Fig. 4.

5. Stimulated Emission

A constant level of stored energy was again maintained by irradiating the phosphor, with uv light, at a spot other than the viewing position. The emission spectra obtained are very similar to the visible excited fluorescence spectra in Fig. 2(c), and they are presented in Fig. 5.

6. Infrared Quenching of Fluorescence

These spectra were obtained by simultaneously irradiating the same area of phosphor with polychromatic uv exciting light and with polychromatic infrared light passed through a Corning 7-56 filter. The results of such simultaneous irradiation were compared to the fluorescent emission. These spectra are shown in Fig. 6. It is seen that the sharp spikes of the fluorescence are quenched, whereas the other regions of the spectra are enhanced by the presence of the infrared.

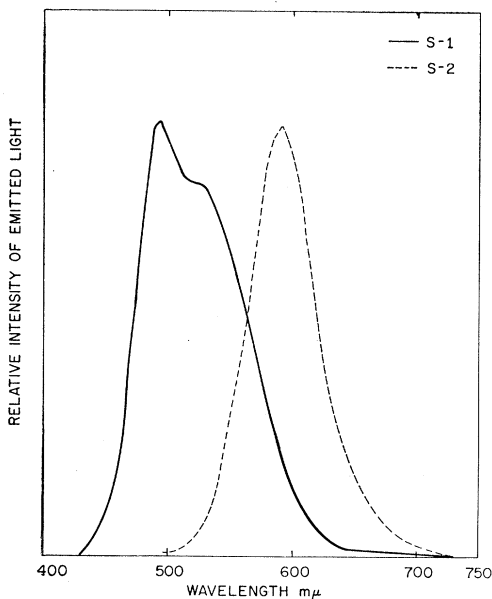


FIG. 5. Stimulated emission.

7. Transmission Measurements

It is important to be able to obtain transmission data in order to determine unambiguously such features as specific absorption peaks and absorption edge. For this measurement one would prefer single crystals. We have grown single crystals of SrS,⁹ and the transmission spectrum is shown in Fig. 7. We have not as yet made single crystals of S-1 or S-2. In the absence of such crystals, one could make a transmission run on the pressed sintered pellets that are used in the photoconductive measurements. The technique of making

⁹ A letter reporting the procedure for growing single crystals and the absorption edge is now in print [Cheroff, Okrasinski, and Keller, *J. Chem. Phys.* **27**, 330 (1957)].

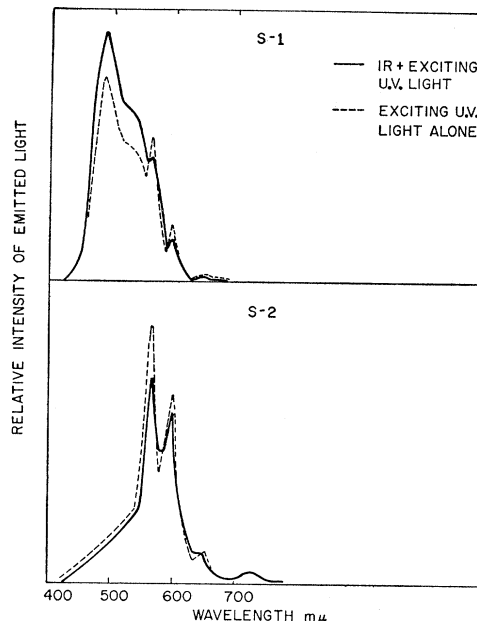


FIG. 6. Infrared quenching of fluorescence.

the pellets is described in the appendix. Since we hope to have single crystals of the phosphors in the near future, we shall postpone the presentation of the transmission spectra of the phosphors.

8. Storage Efficiency

Energy was stored in the phosphor by irradiating the sample with monochromatic exciting light. A constant time of excitation was used for all wavelengths. A measure of the stored energy was determined by detecting the total light output which resulted from the

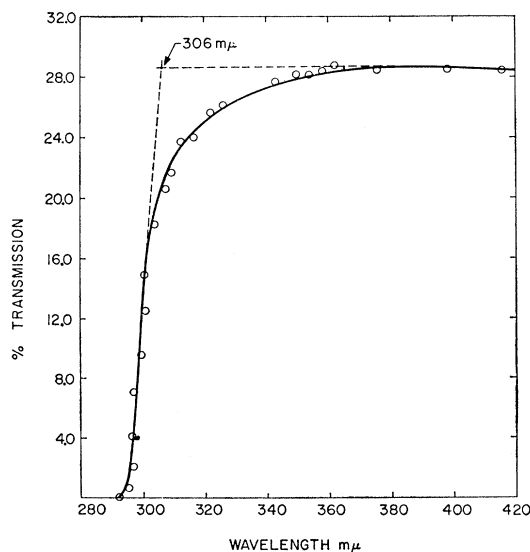


FIG. 7. Transmission spectrum of single crystal of SrS.

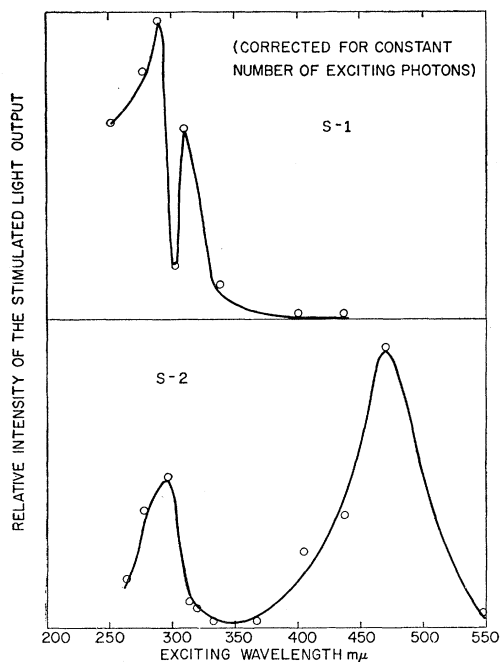


FIG. 8. Wavelength dependence of storage efficiency.

stimulation of the phosphor by infrared light. The maximum value of this measure of stored energy was determined as a function of the wavelength of exciting light. The PE 112U monochromator was varied to allow the irradiation of the sample by a particular wavelength of exciting light, and then by the stimulating light peaked at 1.035μ . The stimulated light output was detected by a 1P21 photomultiplier whose signal was amplified and recorded by a Brush Amplifier and Oscillograph Recorder. The various exciting wavelengths were detected by a thermocouple and a calibration of the relative intensities was made. The results are shown in Fig. 8 where the stimulated light output has been corrected for the intensity and the energy of the exciting radiation, so that the exciting radiation

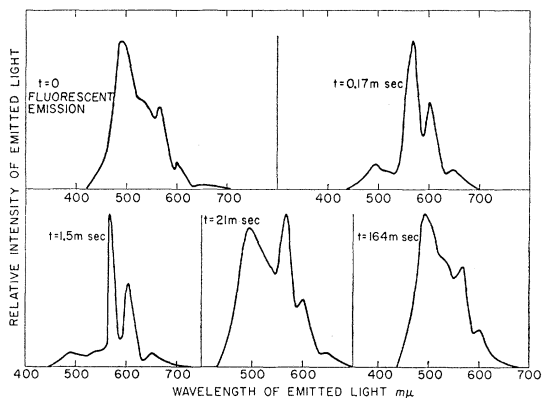


FIG. 9. Phosphorescent spectra of S-1 measured at various times following excitation by $280 m\mu$ light.

was constant in number of photons. In this way, a comparison of the relative heights of the parts of a curve was made meaningful.

9. Tabulation of Energies

From the optical studies, one can construct a table of energies corresponding to structural features of various spectra, such as major peaks and shoulders. Such a compilation of data is presented in Table I.

The data in this table enable us to locate roughly energy levels in a simplified band-theory energy-level diagram. From absorption data of Fig. 7, a measure of the energy gap can be determined. From the fluorescent data, the levels of the primary activator (Ce or Eu) can be located. From the stimulation and the fluorescent spectra, the levels corresponding to the secondary activator (Sm) can be positioned. In the general placement of the various levels, other experimental facts must be considered. A few such facts are the quenching of certain peaks by infrared radiation, the absence of certain structure in the visible excited emission, the gross similarity between the visible excited emission and the stimulated emission, and the relative storage efficiencies. These facts, as well as the results of subsequent sections, will be compiled and utilized in the concluding section of this paper.

B. Time Studies

The instrumentation is described in the appendix.

1. Phosphorescent Studies

The apparatus is shown in Fig. 15. The rotational frequency of the disk was measured by a stroboscope. The angular separation of the two spots was measured and hence the time lapse between excitation and viewing could be determined. We examined the phosphorescence, excited by $280\text{-}m\mu$, $313\text{-}m\mu$, and $436\text{-}m\mu$ light, for the two phosphors.

In the case of S-1, the phosphorescence excited by $313\text{-}m\mu$ light was essentially the same as that excited by the $280\text{-}m\mu$ radiation. The results for $280 m\mu$ are shown in Fig. 9, and it can be seen that the emission is a two-step process, one being relatively fast and responsible for the $490\text{-}m\mu$ peak and the $533\text{-}m\mu$ shoulder, and the other being slower and responsible for the three spikes located at 568 , 600 , and $650 m\mu$. It must be borne in mind that the relative intensities of the various spectra in Fig. 9 decrease rapidly with increasing time, such that the intensity of the spectrum at $t=164$ msec is orders of magnitude less than that at $t=0$. The relative speeds of the two processes can be judged by measuring the ratio of the spike height to the peak height as a function of time. This variation is presented in Fig. 10. The ratio at zero time, namely that during fluorescence, is attained after about 160 milliseconds. The increase of the ratio up to 1.5 msec is due to the

TABLE I. Energies of various optical processes. Values in parentheses indicate minor peaks.

	Excitation		Fluorescence		Phosphorescence		Stimulation		Stimulation emission		Absorption edge	
	ΔE , ev	λ , $m\mu$	ΔE , ev	λ , $m\mu$	ΔE , ev	λ , $m\mu$	ΔE , ev	λ , $m\mu$	ΔE , ev	λ , $m\mu$	ΔE , ev	λ , $m\mu$
SrS	3.94 (4.51)	315 (275)	{ 2.43 510 (3.26 380) averages								3.54-4.05	350-306
S-1	4.39 (3.94)	282 (315)	{ 2.53 490 2.33 533 2.18 568 2.07 600 1.91 650 (3.10) (400)		{ 2.53 490 (2.33) (533) 2.18 568 2.07 600 1.91 650							
	(3.50)	(355)	{ 2.53 490 2.34 531		(2.53) (490) 2.23 556		1.20 1.035		2.53 490 2.33 533			
	2.81	441										
S-2	4.31	288	{ 2.10 ^a 590 ^a 2.18 568 2.07 600 1.91 650 2.33 533 2.10 590		{ 2.10 ^a 590 ^a 2.18 568 2.07 600 1.91 650 (2.33) (533) 2.10 590							
	(4.00)	(310)					1.13 1.094		2.10 590			
	2.64	468										

^a Present in high-fired samples only.

rapid decay of the peak and shoulder relative to the spikes. After that time the decay of the spikes determines the rate of change of the ratio. At 20 msec we see a break in the curve due to the fact that the spikes have decreased to a low level such that the peak and shoulder are again significant. We propose that this is evidence of thermal traps.

At this point we deviate from our avowed procedure and present an interpretation of these results, apart from the general conclusions at the end of the paper. The general conclusion contains the fact that thermal traps are hypothesized but does not involve the detailed interpretation presented here. When there is a constant supply of electrons available in the conduction band, an equilibrium distribution of populated excited states, leading to transitions that result in the spikes and the peak, is obtained and the spike-to-peak ratio is 0.68. There are two sources of populated excited states during phosphorescence. The first population results from electrons excited during fluorescence. The second population results from electrons thermally released from traps that had been filled during excitation. The second population is smaller than the first, and decreases only slowly in time. The first population of those excited states responsible for the peak and shoulder transitions is rapidly depleted during the first 1.5 msec, and it approaches that which is maintained by the emptying of thermal traps. Since the spike transitions are slower, it takes a longer time to get the corresponding decrease of the first population of these states. It is only after 20 msec that the population of these excited levels has nearly reached that which can be maintained

by the slowly decreasing emptying of thermal traps, and it has reached it by 60 msec.

In the case of *S-2*, the uv-excited phosphorescence shows only the spikes and they simply decrease monotonically in time. We note at this point that the 590- $m\mu$ emission in *S-2* is the slowest of all the transitions of both phosphors. The relative speeds of the various processes are significant to the conclusions we present at the end of the paper.

2. Infrared Exhaustion Studies

The term exhaustion curve refers to the time change of the stimulated light output which takes place while the sample is irradiated by a constant infrared radiation after it had been excited by a 2537 Å Hg lamp. These

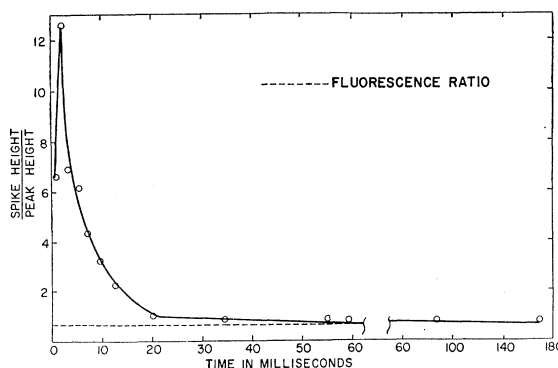


FIG. 10. Ratio of spike height to peak height of the phosphorescent emission of *S-1* for various times after excitation.

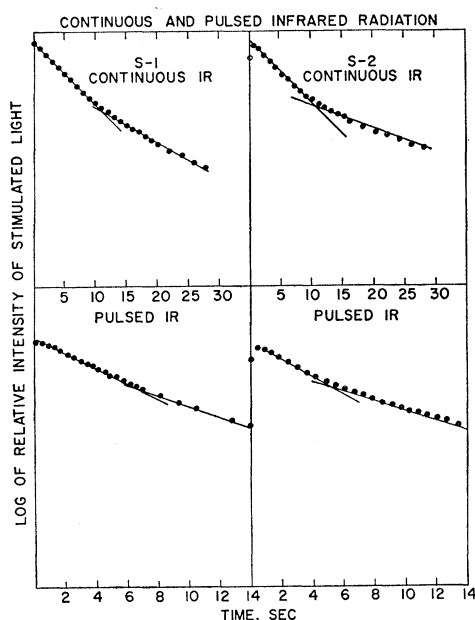


FIG. 11. Exhaustion curves.

curves were obtained with the use of apparatus described in the Appendix. Two types of exhaustion runs were made; one made use of pulsed infrared radiation and the other made use of an uninterrupted beam. The results of a continuous exhaustion and an intermittent exhaustion are shown on semilog plots in Fig. 11. The straight lines indicate exponential decays and the breaks can be interpreted with the assumption that two processes are occurring, each of which is exponential in character. At the break, there is a change in dominance of one of the two processes. One difference between the two processes could be that the first process involves the release of electrons from storage and thermal traps, and the second involves only storage traps. Another difference could be that retrapping is important in the one process and not in the other, and the break in the curve could represent that point where retrapping becomes important.

There are tabulated in Table II the times necessary for the different runs for the intensity of emitted light to decay to half the initial value. Note that the half-times for S-1 appear to be independent of the duty cycle, while they do not for S-2. The half-times appear to be correlated to the breaks in the curves of Fig. 11. It is worth mentioning that the half-times and the breaks in the exhaustion curves are functions of the infrared intensity in that the smaller the intensity the longer will be the time necessary to empty a fixed number of filled traps and hence the longer will be the half-time.

C. Photoconductive Studies

A study of the photoconductive response gives information complementing that information obtained from

spectral and time studies. If the wavelength dependence of photocurrents is found to be coincident with a particular absorption or emission, it indicates that the optical process involves the raising of electrons into a conduction band or the dropping of holes into a valence band, or both. As a result, dc photoconductive measurements were made. Ideally, single crystals of the phosphors should be used for such measurements in order to eliminate spurious effects introduced by grains and grain boundaries and to increase sensitivity. However, workable crystals of phosphors have not yet been obtained, and so powdered samples had to be used. The phosphors were pressed into pellets, sintered, and electroded. The pellets' preparation and characteristics are described in the Appendix. The apparatus for measuring the wavelength dependence of photoconductive response is described in the Appendix. The results are shown in Figs. 12(a) and 12(b). The depicted curves are representations of typical responses of a large number of samples. The spectra coincide very closely with the optical excitations and stimulations shown in Figs. 1 and 4. Hence, one concludes that the excitations in the uv and visible regions, and the stimulations in the infrared region, are accompanied by the motion of either electrons in the conduction band, or holes in the valence band, or both.

II. CONCLUSION

There are certain general observations and conclusions that one can make. As is known, the activators can be classified as either one of two types; the primary such as Eu or Ce, or the secondary such as Sm. It has been thought by workers in the field that the primary activator determines the spectra of the excitation in the visible and the emission, while the secondary activator increases the sensitivity of the phosphor, reduces the phosphorescent afterglow, increases the storageability, and determines the stimulation spectrum. As a result of our investigation, we will conclude that both activators help determine the emission, just as the interplay of both activators determines the region of storage, as well as the storageability. Further, we will

TABLE II. The times necessary for the intensity of emitted light to decay to half the initial value.

Phosphor	Type of run	Pulse width sec	Time between pulses sec	Half-times sec
S-1	Continuous infrared			7.2
	Pulsed infrared	0.12	0.48	7.1
	Pulsed infrared	0.23	0.36	6.8
	Pulsed infrared	1.39	3.3	7.0
S-2	Continuous infrared			8.5
	Pulsed infrared	0.16	0.17	7.0
	Pulsed infrared	0.38	1.10	6.1
	Pulsed infrared	0.40	1.10	5.2

conclude that the primary activator largely determines the afterglow and its rate of decay.

In order to predict further properties and to correlate known properties of the two phosphors at this point, we propose a physical model based upon some simple band-theory considerations for each phosphor. The criteria that we use in evolving these models are (1) consistency with the experimental results described in the preceding sections, and (2) consistency with the known chemical properties of the various constituents in those cases where the chemical properties could be reasonably applied. The activators that are used are rare-earth ions. We do not know whether these ions are maintained in the lattice in substitutional or interstitial sites. The electrons involved in any transition are $4f$ electrons which can be considered to be part of the inner core of the ions. Regardless of whether they are interstitial or substitutional, the inner core of the ions remains relatively undisturbed by the electrostatic field of the lattice. Because of this effective shielding from lattice interactions, one should be able to talk about the activators as if they were isolated ions and to describe them in atomistic language, using such terms as valence state, ionization potential, ground-state term signatures, etc. We assume that the charged ion is sitting at some site. The $+n$ charge on the ion may be due to the fact that n electrons have been distributed to its neighbors for bond formation. Alternatively, the ion could be sitting at some site, polarizing its neighbors, with its electrons contained by an anion located elsewhere in the lattice. It is not within the scope of this paper what the exact nature of the activator site is, nor what the condition of binding is.

In the case of *S-1* the activators are Sm and Ce. It is most likely that each is present in the $+3$ state, and using the Heitler-London approach, the former has a $4f^5$ configuration, while the latter has a $4f^1$ configuration. The probable valence states of gaseous Ce are the $+3$ state and the $+4$ state, the latter with a $4f^0$ configuration. The stability of the unfilled orbital in the latter makes this configuration a likely one as evidenced by the fact that this state is readily found in nature (differing from most of the other rare earths). As a result, it is natural to assume that Ce^{+3} in the lattice would have a low ionization potential and would also be a good hole trap, a property that can shed light on such diverse phenomena as decay rates of phosphorescence and storageability as a function of wavelength. In the case of Sm, possible valence states would be $+2$, $+3$, and $+4$ with $4f^6$, $4f^5$, and $4f^4$ configurations,¹⁰ respectively. There is no one configuration of great stability that would make one stable with respect to another. Hence, Sm^{+3} would be a possible hole trap but not as good a trap as Ce^{+3} . It could also be a possible electron trap since Sm^{+2} is possible. The phosphor *S-2*

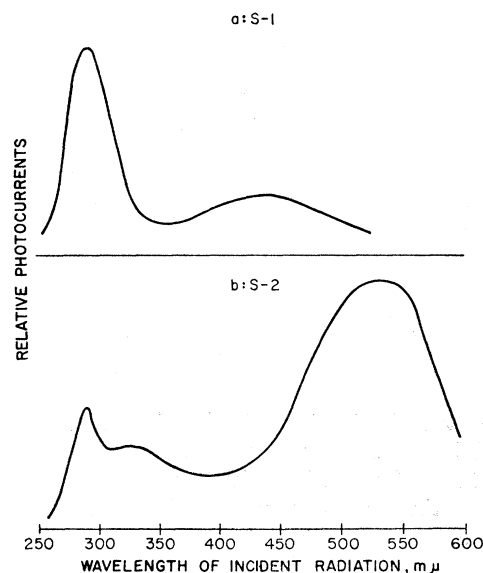


FIG. 12. Wavelength dependence of photocurrents. (a) *S-1*; (b) *S-2*.

has Sm and Eu as activators. Sm again is in the $+3$ state. We propose that the Eu is in the $+2$ state, which is consistent with the reports of Przibram¹¹ and others,¹² and that it has a configuration of $4f^7$. The probable valence states of gaseous Eu are $+2$ and $+3$, the latter with a configuration of $4f^6$. Eu is added in the form of Eu_2O_3 ; however, the material is fired in a reducing atmosphere, and it is the stability of the half-filled orbital that causes the Eu to exist in the $+2$ state. Since Eu^{+3} does readily exist, this valence state is available to Eu and hence we would expect Eu^{+2} to have some ability to trap holes, although not as much as the Ce^{+3} in the case of *S-1*. From this consideration, one can remark on differences between the two phosphors with respect to phenomena such as decay rates of phosphorescence and storageability as a function of wavelength.

In the case of Ce^{+3} , the ground state, according to Hund's rules, is $^2F_{5/2}$. The next state is $^2F_{7/2}$ which, according to Kröger and Bakker¹³ is separated from the ground state by about 0.22 eV. This doublet leads to the appearance of the shoulder and peak in the various emissions. These facts and conclusions will be utilized in the discussion of the model, presented in Fig. 13, in which only those levels are presented that lead to the salient optical characteristics. Levels due to accidental impurities are omitted. In the case of Eu^{+2} the ground state is $^8S_{7/2}$. Since the $^8S_{7/2}$ lies alone, the emission contains only one peak. The model for *S-2* is depicted in Fig. 14. (As implied earlier, we do not consider the crystal field splitting of these levels. The effect of the crystalline field will be discussed in a future paper.)

¹⁰ We omit from consideration the possibility of $6s$, $6p$, and $5d$ orbitals being occupied in place of one of the $4f$ orbitals. This possibility is not important to the results of the work.

¹¹ K. Przibram, *Acta Phys. Austriaca* 3, 126 (1949-1950).

¹² W. Low, *Phys. Rev.* 98, 2, 426 (1955).

¹³ F. A. Kröger and J. Bakker, *Physica* 8, 628 (1941).

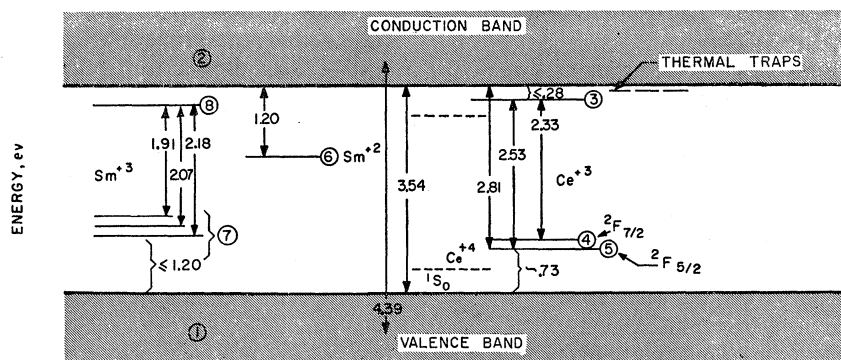


FIG. 13. Model for S-1.

The uv excitation in both phosphors corresponds to the SrS base absorption and it results in electrons being excited from 1 to 2 with holes being left in the valence band. In this process, any of the following three processes can and do occur:

(1) For S-1, a hole is trapped by levels 4 and 5 of Ce^{+3} which becomes Ce^{+4} whose levels are shown dotted in Fig. 13. The Ce^{+4} can then trap an electron and become Ce^{+3} with the proper rearrangement of levels, the electron populating level 3. In this manner we have started with a Ce^{+3} in a ground state with the electron in question occupying level 5 and we have ended with Ce^{+3} in an excited state with the electron in level 3. This is followed by transitions 3→4 and 3→5 which are responsible for the shoulder and peak in the fluorescence. In the process, Ce has gone from +3 to +4 and thence back to +3. The efficiency of Ce^{+3} as a hole trap coupled with the ability of Ce^{+4} to trap electrons necessitates the recombination transitions to be rapid. For S-2, a hole is trapped by level 4 of Eu^{+2} which becomes Eu^{+3} . Because of the stability of Eu^{+2} , this occurs with less probability than did the hole trapping by Ce^{+3} . In the low-fired samples, there is little or none of this since the transition 3→4 is not observed. In the high-fired samples, one does observe this transition, hence some hole trapping by Eu^{+2} does occur. This is probably due to the inclusion of more Eu^{+2} centers in the high-fired samples. Where the 590-m μ peak does occur (i.e., high-fired samples), the Eu has gone from a +2 to a +3 to a +2 excited state and then back to a

+2 normal state, during which a hole and then an electron is trapped with subsequent recombination. Because the holes are not trapped efficiently, the holes and electrons can remain free in the vicinity of the site for a longer time than in the case of the Ce site, thus accounting for the slower rate of decay of phosphorescence of the 590-m μ peak.

(2) A hole is trapped by levels 7 of Fig. 13 or levels 6 of Fig. 14 of Sm^{+3} which becomes Sm^{+4} . This is followed by an electron dropping from the conduction band to an excited state of Sm^{+4} which becomes Sm^{+3} with a readjustment of levels so that the electron in level 8 of Fig. 13 or level 7 of Fig. 14 recombines with the hole in levels 7 of Fig. 13 or 6 of Fig. 14, representing a transition from an excited state of Sm^{+3} to the ground state. The net result is the appearance of the three spikes during the fluorescence. Of course, a change in the order of events equally well explains the emission, i.e., an electron could be trapped by an Sm^{+3} leading to an occupied Sm^{+2} level 6 (or level 5 of Fig. 14). A hole could then be trapped by this center resulting in a Sm^{+3} in an excited state which in turn results in a transition to the ground state with the emission of the three spikes. The Sm^{+3} level must lie beneath the Sm^{+2} to satisfy the fact that the former has a higher ionization potential. How much beneath it lies would be dependent on how big an effect the dielectric constant of SrS has on the ionization potentials of Sm. They are certainly reduced from the values in the gaseous state. The size of the reduction depends on the ineffectiveness of the

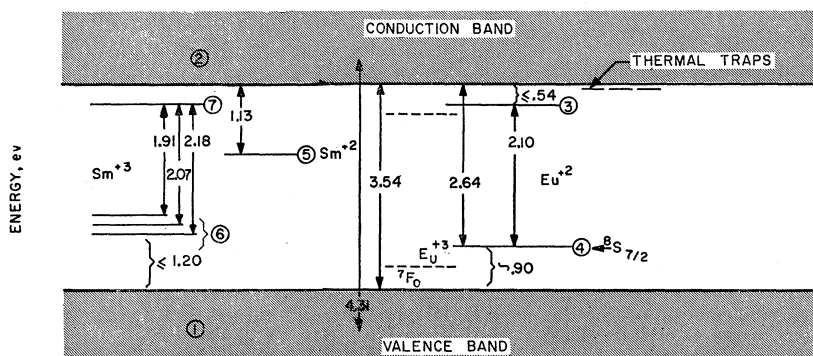


FIG. 14. Model for S-2.

shielding of the dielectric base material from the rare-earth impurity. The Sm^{+2} ionization potential in SrS is given by the distance of level 6 of Fig. 13 or 5 of Fig. 14 from the conduction band, or about 1 ev. In the gaseous state, the third ionization potential of Sm is about 20 ev and the fourth is about 35 ev. If one assumes the same effective dielectric constant for the case of Sm^{+2} as for Sm^{+3} , the Sm^{+3} level might be expected to lie about 0.8 ev below that of Sm^{+2} . This is undoubtedly too small a difference but, on the other hand, a very large difference need not be expected.

(3) An electron in the conduction band becomes trapped in a Sm^{+3} site. The site then becomes Sm^{+2} and is shown as level 6 of Fig. 13 or 5 of Fig. 14.

The net effect in the uv excitation is that an electron has been stored by Sm and the corresponding hole has become trapped by Ce or Eu (Ce^{+3} and Eu^{+2} are more effective at trapping holes than Sm^{+3}). During the infrared quenching described in Sec. I-6, electrons are excited in *S-1* from 1 to 7 and in *S-2* from 1 to 6 which action can neutralize a hole that had been trapped there, and hence the spikes caused by transitions 8→7 of *S-1* or 7→6 of *S-2* are quenched, and in the case of *S-1* the peak and shoulder produced by transitions 3→4 and 3→5 are correspondingly enhanced. According to this picture, the uv excitation should be efficient at storing energy in both phosphors and it is indeed, as shown in Fig. 8. One might wonder why a phosphor with Sm alone, as an activator, does not store energy and why Ce or Eu must be included. From the above, it is seen that the role of the Ce or Eu, is to trap holes and thus to cut down the probability of band-to-band and other recombinations, which does occur in SrS, as shown earlier in the fluorescence spectra of Fig. 2(a). With holes trapped by Ce or Eu, the probability of electrons being stored in Sm sites is greatly enhanced. In the case of *S-1* the rapid rates of decay of the 3→4 and 3→5 transitions are due to the readiness of Ce^{+3} to trap a hole and the effectiveness of Ce^{+4} to trap an electron with the recombination process being within the Ce^{+3} site and being very rapid. On the other hand, in *S-2*, the relative slowness of the rate of decay, during phosphorescence of 3→4 is due to the fact that the hole-trapping ability of Eu^{+2} is less than that of Ce^{+3} . Sm^{+3} is less effective at trapping holes and hence holes can remain in the environs of Sm^{+3} without being effectively trapped resulting in a slower rate of decay in the resultant 8→7 transitions. The uv photoconduction observed presumably would be due to motion of electrons in the conduction band with but a small contribution from hole motion. The fact that the uv photoconduction of *S-1* is small compared to *S-2* is due to the rapid hole-electron recombination via the Ce^{+3} site whereas holes and electrons have longer lifetimes in *S-2*. The existence of thermal traps produces the observed uv-excited phosphorescence.

For *S-1*, the blue excitation involves the excitation of an electron from 5 to 2. This automatically leaves

a hole trapped on the site resulting in Ce^{+4} . Since this eliminates the trapping of holes by Sm^{+3} , there are no spikes present. In time there could be a redistribution of hole population so that some would be trapped by Sm^{+3} , as manifested by the appearance of weak spikes in the blue-excited phosphorescence. Since the hole is created on the Ce site, the electron can very easily be trapped in level 3 with a rapid recombination leading to the rapid 3→4 and 3→5 transitions. Because of the effectiveness of the Ce as a hole trap, the excited electron has little chance to get widely separated from the center and hence there is little probability of the electron being trapped by a Sm site. And so one measures only slight storageability in the blue region of the spectrum. Similarly, the photoconductivity in this region is not too great (when compared to *S-2* in this region). For *S-2*, the blue excitation involves the excitation of an electron from 4 to the conduction band. This leaves a hole trapped on the site resulting in a Eu^{+3} . This trapped hole perhaps can be thermally released into the valence band and so the electron-capture cross section for the center on a time average will be smaller than that for the Ce^{+4} in *S-1*, in which there was little probability for the trapped hole to be thermally released into the valence band. Hence, the lifetime of excited conduction electrons is long resulting in their capture by an Sm site and in the occupation of level 5 with concomitant storage of energy. Owing to the low capture cross section for holes of Eu^{+2} , some of the Eu^{+3} might become converted to Eu^{+2} , with the hole being trapped by levels 6 followed by the capture of an electron and subsequent recombination resulting in the spikes of 7→6. This explains the appearance of weak spikes during the fluorescence excited by 436 m μ , which differs from the observations for *S-1*. This also explains the appearance of spikes in the blue-excited phosphorescence. As a result of these considerations, the slow decay times of the 590-m μ emission, caused by 3→4, during phosphorescence can be understood. The long lifetime of the electrons, as well as the presence of some holes in the valence band, explains why the photoconduction during blue excitation is so large (compared to that of *S-1*). The long lifetime of the conduction electrons leads to the prediction that the blue region of the spectrum should be efficient at storing, and this is found to be the case, which again differs from that of *S-1*. The existence of the thermal traps explains the occurrence of blue-excited phosphorescence which is quite weak, as expected from the above considerations, and is much weaker than that excited by uv. The blue-excited phosphorescence of *S-2* is stronger than that of *S-1*, as one would expect from the above considerations.

The infrared stimulation is that process in which the electron leaves level 6 of Fig. 13 or level 5 of Fig. 14 and the Sm^{+2} becomes an Sm^{+3} . In the case of *S-1*, the freed electron will move through the conduction band until it is attracted to a trapped hole in an Ce^{+4} site.

At this point, the electron drops into a level which then becomes level 3 of the Ce^{+3} and both 3→4 and 3→5 transitions result. Most of the holes that had been formed in excitation would have finally been trapped by Ce^{+3} and hence essentially only the typical peak and shoulder arise upon stimulation.¹⁴ In the case of *S-2*, the freed electron will be attracted to a trapped hole in a Eu^{+3} site. At this point, the electron drops into the excited state of Eu^{+3} , and there is a rearrangement of levels to that of Eu^{+2} with the transition 3→4 resulting. We have not observed spikes in the stimulated emission in spite of the fact that one expects holes to be redistributed such that some become trapped by 6. (This could be due to the conditions of the experiment in which we measure this emission. We simultaneously irradiate a rotating wheel with ultraviolet and infrared light when we measure the stimulated emission. Hence, only a small period of time is allowed to elapse between excitation and stimulation in which time there has been little opportunity for hole redistribution.) During the stimulation of both phosphors, one observes a photocurrent due to electron motion which decays in time.

It is worth noting that the difference in energy of the two transitions 3→4 and 3→5 is 0.20 eV, to be compared with the average value of 0.22 eV given by Kröger and Bakker.¹³

The Sm^{+2} level is closer to the conduction band in *S-2* than in *S-1*. This is perhaps due to perturbations on the energy gap by Eu differing from those of Ce.

From the above considerations one can make predictions about possible optical transitions, quenchings, stimulations, etc. As an example, we plan to look for the emission corresponding to either 7→1 in Fig. 13 or 6→1 in Fig. 14 which occurs during hole trapping by Sm^{+3} . One might observe a similar emission corresponding to transitions 4, 5→1 in Fig. 13 or 8→1 in Fig. 14 during the hole trapping of Ce^{+3} or Eu^{+2} , respectively. As for the quenching experiments, we plan to look carefully for the transitions 1→4, 5 and 1→7 in Fig. 13 and 1→4 and 1→6 in Fig. 14, as well as for their effects on uv-excited and blue-excited fluorescence.

One can further make predictions about different phosphors based upon the atomic structure of the activators. Thus, one would expect a phosphor containing Sm and Tb as activators to be similar to *S-1*. Tb^{+3} with a $4f^8$ configuration¹⁰ and a ground state of 7F_6 would be a good hole trap since Tb^{+4} has a stable configuration of $4f^7$ with a ground state of $^8S_{7/2}$. As a result, one would predict that the decay rate of phosphorescence would be rapid and that this phosphor would store mainly in the uv. Similarly, one would expect a phosphor with Sm and Yb to be similar to *S-2*. Yb^{+2} with a $4f^{14}$ configuration¹⁰ and a ground state of 1S_0 would not be

a good hole trap, and so the rate of decay of phosphorescence would be slow and the phosphor would store in the blue as well as in the uv. These phosphors have been made and the spectra and properties are under investigation.

APPENDIX

I. Chemical and Materials Preparation

The materials were prepared in this laboratory with the use of procedures that, to a large extent, have been worked out elsewhere.^{1, 2, 15-17}

SrS was obtained by firing purified $SrSO_4$ in H_2 at 1000°C for an hour. Purified $SrSO_4$ was obtained with a procedure outlined elsewhere.¹⁶ The $SrSO_4$ was analyzed for impurities on a Jarrell-Ash spectrograph. Small traces of Ba, Ca, and Na but no traces of Cu and other common contaminants were found. When the $SrSO_4$ was reduced in a quartz or an alundum boat, the resultant SrS contained Cu and/or Al impurities. However, when the quartz boat was lined with Pt foil, the resultant SrS was free from such detectable contamination.

The phosphors investigated in this study were prepared with the SrS which had no detectable trace impurities of anything except Na and Ba. *S-1* consisted of SrS, 6% $SrSO_4$, 6% CaF_2 , 0.02% Ce, and 0.02% Sm. *S-2* consisted of SrS, 6% $SrSO_4$, 6% CaF_2 or 6% NaCl, 0.02% Eu, and 0.02% Sm. The percentages are expressed in terms of molar percent. The CaF_2 and NaCl acted as flux. The materials were intimately mixed and dried, and were ready for subsequent firing.

For the optical and the time studies, the dried materials were heated in H_2S for two hours at 1100°C in quartz boats. The fired materials were then ground, sieved, and sprinkled on a surface that had been wetted with a 0.1% solution of Duco cement in amyl acetate. (It was determined that this amount of Duco cement did not alter any of the measurements.)

In order to measure the dc photoconductive response, the resistivity of the samples had to be kept as low as possible. Since single crystals were not available at that time, measurements were attempted unsuccessfully on the normal phosphor powders described in the previous paragraph. As a result, the unfired mixtures were pressed into pellets and then fired in order to encourage grain growth. Metal dies and nylon-capped metal dies were first tried but metal impurity contamination proved to be quite high. An all-quartz die was used which eliminated the contamination. Various pressures, atmospheres, lengths of time of firing, temperatures (between 1000°C and 1600°C), and boats

¹⁴ In the case of blue phosphorescence, we stated spikes were present due to small redistribution of holes to Sm levels. In the stimulated emission there also may be the same redistribution, but the effect of the large excess of holes in Ce centers completely masks any possible spikes.

¹⁵ Primak, Osterheld, and Ward, J. Am. Chem. Soc. **69**, 1283 (1947).

¹⁶ Smith, Rosenstein, and Ward, J. Am. Chem. Soc. **69**, 1725 (1947).

¹⁷ K. F. Stripp and R. Ward, J. Am. Chem. Soc. **70**, 401 (1948).

were tried. The procedure that was finally settled upon involved a total pressure of about 7000 psi, a H_2 atmosphere, one-half hour firing time, $1400^\circ C$ firing temperature, and dense alundum boats. In the case of phosphor S-2, CaF_2 was used as the flux since this proved to be more efficient at stimulating grain growth than NaCl. This procedure produced grains whose average size was about 100 microns. The pellets were then electroded with cold-setting silver paste.

A question that we faced quite early was whether or not the different methods of sample preparation, on the one hand the method of pellet preparation and on the other hand the method of powder sample preparation, resulted in like phosphors. If so, the optical and the time measurements could be correlated with the photoconductive measurements. We had to answer such questions as what was the effect of grinding the phosphor, what was the effect of the difference in temperatures and atmospheres of the firings, and what influence did possible contamination from the boat have on the optical properties of the phosphors. To answer these questions, we prepared many different samples and determined the spectra of the emissions at principle exciting wavelengths. To check the influence of grinding, spectra were measured after successive grindings. The grinding changed the height of some sharp spikes, on the emission curve, relative to the remainder of the emission curve, but not seriously. The high temperature of the pellet firing increased the chances of accidental contamination but also produced more sensitive phosphors. The optical properties of an uncontaminated high-fired pellet were very similar to those of a low-fired powdered sample. Firing in H_2 or in H_2S gave very similar samples. To check the effect of contamination from boats, the spectra of samples fired on Mo, alundum, quartz, boron nitride, and MgO were correlated with spectrographic analyses for specific impurities of Al, Mo, B, Mg. They were also compared to spectra of phosphors made with purposely added amounts of these materials as contaminants. The results showed that phosphors fired on quartz at low temperatures were essentially the same optically as those fired on alundum at high temperatures. The other boats were undesirable in that they introduced impurities that changed the optical properties of the phosphors. We also looked for changes in optical properties as we changed the flux from CaF_2 to NaCl, but no changes were found. As a result of these comparisons and correlations, we concluded that the powdered samples prepared for optical and time studies were essentially the same as those pellets prepared for photoconductive measurements and hence correlation of results can be made justifiably.

II. Instrumentation

A. Optical Studies

During the early work many variations in the arrangement of the source, the monochromator, and the sample

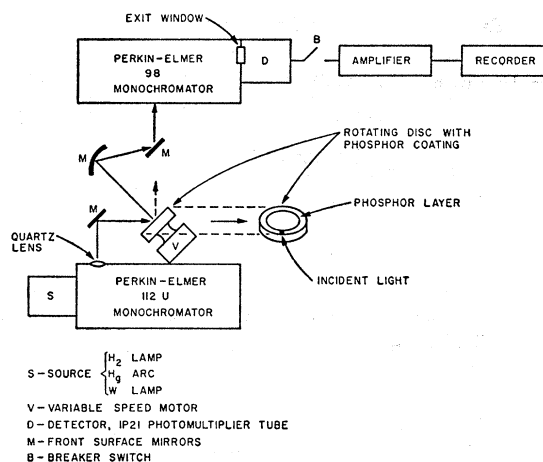


FIG. 15. Optical instrumentation.

were tried. The chief problem was to obtain an arrangement whereby a sufficiently intense monochromatic beam of light was incident on the sample, the attendant stray light was held to a minimum, and a sufficient fraction of the phosphor emission was analyzed and received by the detector. There were other measurement problems which were solved by the optical system developed. One such problem was the maintenance of the sample at a constant level of excitation while stimulation and stimulated-emission spectra were being determined. Without this constant level of excitation, the exhaustion of the stored energy, in the phosphor, during the runs, would lead to spurious results and false conclusions. This system was a versatile two-monochromator apparatus in which the phosphor powder was mounted as a peripheral ring on a disk that could be rotated. The setup is shown in Fig. 15. The probable errors in wavelength due to reproducibility, calibration, slit widths, etc., amounted to ± 1 to $\pm 2 \mu$ over the spectrum covered.

Chopped monochromatic radiation from the PE 112U monochromator is focused onto the phosphor film. The phosphor emission is focused into the PE 98 monochromator. The pulsed signal from the detector is amplified and recorded by the PE 112U system. B, in Fig. 15, is a relay operated by a battery and the PE 112U signal breaker. The relay breaks the circuit to the amplifier during the time that the 112U beam chopper interrupts the light beam. B is required for phosphorescence measurements and for excitation and fluorescence measurements where the phosphorescent decay is slow. In this way, we discard the phosphorescence which would otherwise reach the amplifier out of phase with the fluorescent signal and hence subtract from it.

The way in which this system was used to determine and record the various types of spectral data is summarized in Table III. In the excitation-spectra measurements, the hydrogen and tungsten lamps were used as sources, whereas in the fluorescent-spectra measure-

TABLE III. Procedure for recording spectral data.

Type of spectrum	PE 112U setting	Disk	PE 98 setting
Excitation	Scanned	Still	Fixed at peak emission λ
Fluorescence	Fixed at exciting λ	Still	Scanned
Phosphorescence	Fixed at exciting λ	Rotated ^a	Scanned
Stimulation	Scanned	Rotated ^b	Fixed at emission λ
Stimulated emission	Fixed at stimulating λ	Rotated ^b	Scanned

^a The exciting beam is incident upon the sample in advance of the viewing position.

^b An additional exciting radiation is incident upon a spot away from the viewing position.

ments a Hg arc lamp was used. In the phosphorescence investigations, the PE 112U beam chopper was removed and the exciting radiation was focused on a point in advance of the viewing position. As the disk rotated, the sample was moved from the exciting beam to the viewing point where the phosphorescence was recorded, the relay *B* being used to interrupt the dc signal.

For the infrared stimulation and stimulated-emission spectra measurements, the phosphor was held at a constant level of excitation during the measurement by rotating the disk while an additional source of exciting radiation was incident at a point away from the viewing point. Infrared stimulating radiation from the PE 112U with tungsten source was focused onto the viewing position.

B. Time Characteristics

In the measurement of change in phosphorescent spectrum as a function of time, the experimental setup was the same as that shown in Fig. 15. The exciting light from the PE 112U struck the phosphor at a spot

in advance of the spot viewed by the PE 98. The rotational frequency of the disk was variable and was measured with a stroboscope. From the measured frequency and the known angular separation of the two spots, the time lapse between excitation and viewing was calculated. The speed of the disk could be varied between 10 rpm and 13 000 rpm. The angular separation between the exciting and the viewing spots was 10°. The time delays between excitation and viewing phosphorescence varied between 0.13 and 165 milliseconds.

A second type of time measurement involved the exhaustion of the stored energy of the phosphor. This was effected by irradiating the sample with chopped or steady infrared radiation. This method utilized a light chopper which presented a trapezoidal light pulse of a variable width and of a variable frequency with a 100-microsecond rise and decay time. Infrared light, from a Nernst glower, was passed through a Corning 7-56 infrared-transmitting filter and through the chopper and was incident on the phosphor slide. The total light emitted was detected by a 1P21 photomultiplier tube whose signal was amplified by a Brush amplifier (dc to 120 cps response) and was recorded on a Brush oscillograph recorder.

C. Photoconductive Studies

The apparatus contained a Beckman Model DU monochromator whose light source was a high-pressure Xe arc lamp, which supplied continuous radiation in the region under investigation. The phosphor pellet was situated so that the electrodes were on the irradiated surface, perpendicular to the cylindrical axis of the pellet. The interelectrode spacing was between 1 and 3 mm. The photocurrents were measured with a Beckman vibrating reed micromicroammeter.